

# Fuzzy Hopfield neural network with fixed weight for medical image segmentation

Chwen-Liang Chang

Yu-Tai Ching, MEMBER SPIE

National Chiao Tung University

Department of Computer and Information

Science

Taiwan

**Abstract.** Image segmentation is a process for dividing a given image into meaningful regions with homogeneous properties. A new two step approach is proposed for medical image segmentation using a fuzzy Hopfield neural network based on both global and local gray-level information. The membership function simulated with neuron outputs is determined using a fuzzy set, and the synaptic connection weights between the neurons are predetermined and fixed to improve the efficiency of the neural network. The proposed method needs initial cluster centers. The initial centers can be obtained from the global information about the distribution of the intensities in the image, or from prior knowledge of the intensity of the region of interest. It is shown by experiments that the proposed fuzzy Hopfield neural network approach is better than most previous approaches. We also show that the global information can be used by applying the hard *c*-means to estimate the initial cluster centers. © 2002 Society of Photo-Optical Instrumentation Engineers. [DOI: 10.1117/1.1428298]

Subject terms: medical image segmentation; fuzzy clustering; Hopfield neural network.

Paper 010071 received Feb. 27, 2001; revised manuscript received July 19, 2001; accepted for publication July 20, 2001.

## 1 Introduction

Image segmentation, a process to divide a given image into meaningful regions with homogeneous properties, is an essential step in image analysis and recognition. A large number of algorithms, for example Refs. 1–3, have been proposed in the past. Those conventional image segmentation algorithms can be categorized generally into three classes: (1) histogram-based schemes, where the pixels are segmented into classes based on overall gray levels; (2) region-based schemes, by which homogeneous properties around a given pixel are enlarged; and (3) edge-based schemes, which detect the pixels with abrupt changes in gray levels, and then connects selected pixels to form completely enclosed boundaries.

Recently, neural network-based architectures<sup>4–11</sup> have been applied for image segmentation. Dhawan and Arata<sup>4</sup> proposed a two-dimensional self-organizing feature map-based approach that incorporates both local and global information about the gray-level distribution of the image, and explores the useful features of the image to determine and extract meaningful regions of interest. They used the concept of competitive learning to find the overall gray-level distribution of the image as the global information. A contrast measure defining the homogeneity of the region was also used as the local information. In Refs. 5 and 6, the image segmentation process was formulated as a constraint satisfaction problem (CSP) by interpreting it as a process of assigning labels to pixels. A three-dimensional constraint satisfaction neural network was developed to form the constraints in the CSP. A method using a competitive Hopfield neural network (CHNN), based on the global gray-level values distribution, was proposed by Cheng, Lin, and Mao.<sup>7</sup> The problem of image segmentation is regarded

there as minimization of a cost function, which, in turn, is defined as the mean value of distance measures between the gray-level values and the members of classes. Lin, Cheng, and Mao<sup>8</sup> proposed a fuzzy Hopfield neural network (FHNN), based on the pixel classification, for image segmentation. This approach added a fuzzy reasoning strategy into a neural network. In FHNN, the process of image segmentation is also regarded as a minimization problem in which the cost function is defined as the Euclidean distance between the gray levels in a histogram and the cluster centers represented in the gray levels. In general, those methods for medical image segmentation make use of the local information, i.e., the gray-level values of the neighborhood pixels, or the global information, i.e., the overall gray-level distribution in the image.

In medical image segmentation, the half volume effect in CT images and the noise in ultrasound images are typical difficulties encountered. The local information-based method cannot correctly find the boundary when the half volume effect is significant. The global information-based method cannot work correctly when there is significant noise, as in ultrasound images. We propose a segmentation algorithm that incorporates both local and global information for medical image segmentation. First, the global gray-level information is used to segment the image for the initial partition, and then local information is used to construct a Hopfield neural network, to simulate the membership function. Each neuron corresponds to a pixel in the image. A pair of neurons are connected if they are neighbors in the image, and the synaptic connection weights are predetermined and fixed to improve the efficiency. Second, the fuzzy set approach is applied and a defuzzification process is triggered to determine the outputs of the neurons; and

when the network converges into a stable state, the association of a pixel to a cluster is decided.

The remainder of this work is organized as follows. The hard  $c$ -means and fuzzy  $c$ -means algorithms are reviewed in Sec. 2, and the fuzzy Hopfield neural network with the fixed-weight approach is described in Sec. 3. In Sec. 4, we present the results obtained by the proposed algorithm. Conclusions are given in Sec. 5.

## 2 Hard $c$ -Means and Fuzzy $c$ -Means Algorithms

The hard  $c$ -means and the fuzzy  $c$ -means algorithms are well known for classification of points in space into clusters. When these algorithms are applied for image segmentation, the pixels with similar intensity are gathered into clusters to identify the region of interest. In this section, these algorithms are briefly described for completeness. The details can be found in Ref. 12.

### 2.1 Hard $c$ -Means Algorithm

A set of  $n$  points is denoted as  $X = \{x_1, x_2, \dots, x_n\}$  in space. Suppose we divide the set of points into  $c$  clusters. It is said that the matrix  $U = [u_{ik}] \in M_{nc}$  is a hard  $c$ -partition of  $X$  if it satisfies the following conditions:

$$\sum_{k=1}^c u_{ik} = 1,$$

$$\sum_{i=1}^n u_{ik} < n, \quad \text{and}$$

$$\sum_{i=1}^n \sum_{k=1}^c u_{ik} = n,$$

where  $u_{ik} \in \{0, 1\}$ .

The procedure of the hard  $c$ -means algorithm is summarized in the following steps.

1. Choose a primary set of  $c$  points,  $\{v_k | k = 1, 2, \dots, c\}$  as the cluster centers.
2. Calculate the membership matrix  $U$  based on the minimum Euclidean distance as follows:

$$u_{ik} = \begin{cases} 1, & \text{if } (\|x_i - v_k\|)^2 = \min_{j=1}^c \{(\|x_i - v_j\|)^2\} \\ 0, & \text{otherwise} \end{cases}, \text{ for all } i, k.$$

3. Update the new cluster centers  $\hat{v}_k$ ,

$$\hat{v}_k = \frac{\sum_{i=1}^n (u_{ik})(x_i)}{\sum_{i=1}^n u_{ik}}.$$

4. If  $\hat{U} = U$  then stop; otherwise go to step 2.

The hard  $c$ -means algorithm is easy to implement. But it is sensitive to the noise in the image.

### 2.2 Fuzzy $c$ -Means Algorithm

The hard  $c$ -means algorithm allows a point to belong to only one cluster. But in the fuzzy  $c$ -means algorithm, every point belongs to all clusters with different degrees of the membership functions. The conditions of the membership matrix  $U$  of the fuzzy  $c$ -means are modified as follows:

$$\sum_{k=1}^c u_{ik} = 1, \quad 1 \leq i \leq n,$$

$$\sum_{i=1}^n u_{ik} < n, \quad 1 \leq k \leq c, \quad \text{and}$$

$$\sum_{i=1}^n \sum_{k=1}^c u_{ik} = n,$$

where  $0 \leq u_{ik} \leq 1$ .

The procedure of the fuzzy  $c$ -means algorithm is summarized in the following steps.

1. Choose a set of points,  $\{v_k | k = 1, 2, \dots, c\}$ , as the initial cluster centers.
2. Calculate membership matrix  $U$  for all points to all clusters using the following equation.

$$u_{ik} = \frac{[ \|x_i - v_k\|^{-2} ]^{1/q-1}}{\sum_{j=1}^c [ \|x_i - v_j\|^{-2} ]^{1/q-1}}.$$

3. Update the new cluster centers  $\hat{v}_k$ ,

$$\hat{v}_k = \frac{\sum_{i=1}^n (u_{ik})^q x_i}{\sum_{i=1}^n (u_{ik})^q}.$$

4. If  $\max_{ik} |\hat{v}_k - v_k| < \epsilon$ , where  $\epsilon$  is a stop criterion, then we stop the iteration. Otherwise the iteration restarts at step 2.

The fuzzification factor,  $q$ , a given real number which is greater than 1, decides the convergence speed and the sensitivity to noise. If  $q$  is set to  $1^+$ , then it converges quickly and is less sensitive to the noise. On the other hand, if  $q$  is set to a large number, it will converge slowly and will be more sensitive to the noise.

## 3 Proposed Method

In this section, we present the proposed fuzzy Hopfield neural network with a fixed weight model to simulate the membership matrix for image segmentation. Each pixel in the image is a point in the plane. If there are  $n$  pixels to be divided into  $c$  clusters, then each pixel has  $c$  neurons associated with it. There are  $n \times c$  neurons in this network. Similar to that in FCM, the outputs of the neurons, denoted  $O = o_{ik}, 0 \leq i \leq n, 1 \leq k \leq c$ , form a membership matrix. A membership corresponds to a partition if it satisfies the following conditions:

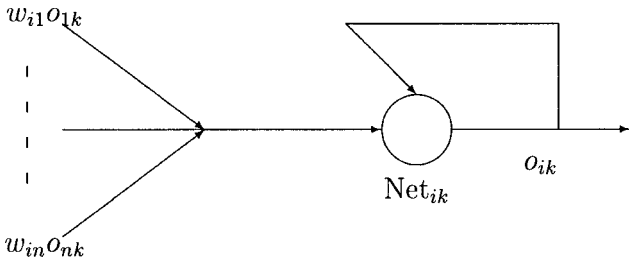


Fig. 1 The structure of a neuron.

$$\sum_{k=1}^c o_{ik} = 1, \quad \text{for all } i,$$

$$\sum_{i=1}^n o_{ik} < n \quad \text{for all } k, \quad \text{and}$$

$$\sum_{i=1}^n \sum_{k=1}^c o_{ik} = n,$$

where  $0 \leq o_{ik} \leq 1$ . Two neurons are neighbors to each other if their corresponding pixels in the image are neighbors to each other. As shown in Fig. 1, each neuron receives contributions from the neighboring neurons and itself as its input. These contributions are weighted by the synaptic weights  $W$ . In our approach, the synaptic weights are fixed and should be determined first. The synaptic weight between two neurons  $i$  and  $j$  is determined by the Euclidean distance, and the similarity of their intensities in the image is as shown in the following equation.

$$w_{ij} = \frac{1}{\alpha_1 [\Delta I(i,j)]^2 + \alpha_2 [D(i,j)]^2}. \tag{1}$$

In Eq. (1),  $\Delta I(i,j)$  is the difference in intensity between pixel  $i$  and  $j$ , and  $D(i,j)$  is the Euclidean distance between pixel  $i$  and  $j$ .  $\alpha_1$  and  $\alpha_2$  are the weights to balance these two factors.

The proposed method requires a set of initial cluster centers. The initial cluster centers do not need to be exact, but they should not be far away from the true centers. The initial cluster centers can be either given by user assists or obtained from the global information about the gray-scale distribution of the image. In most of the cases for medical image segmentation, the intensities of the regions of interest are known. Users can provide the cluster centers from such available knowledge. Otherwise, the cluster centers can be estimated using a  $c$ -means method.

Given a set of  $c$  initial cluster centers, we perform the initial partition as:

$$o_{ik}^{(0)} = \frac{\{1/[I(i) - v_k]^2\}^{1/q-1}}{\sum_{j=1}^c \{1/[I(i) - v_j]^2\}^{1/q-1}}, \quad 1 \leq i \leq n, 1 \leq k \leq c,$$

where  $I(i)$  and  $v_k$  are, respectively, the intensity values of pixel  $i$  and the  $k$ 'th class center.

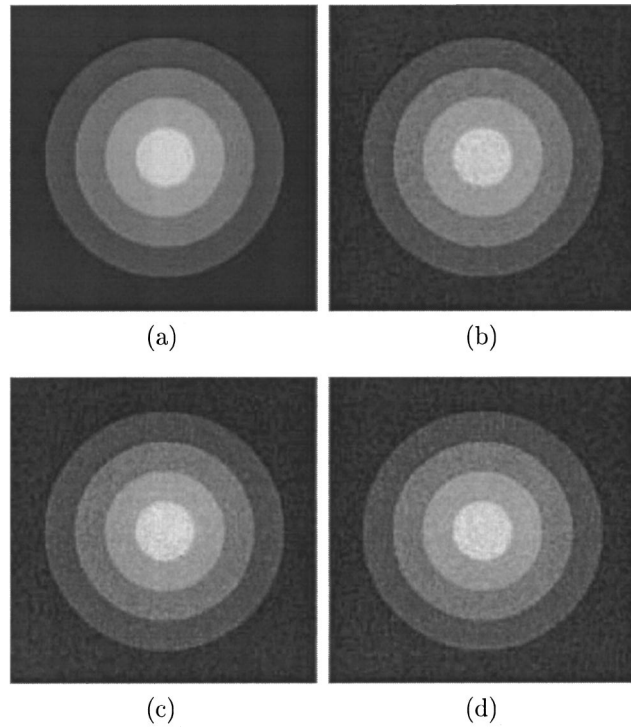


Fig. 2 The simulated image with (a) a constant gray level in background and each disk; (b), (c), and (d) are the simulated images with added noise levels  $K=20, 23,$  and  $25,$  respectively.

Recall that a neuron receives outputs from neighboring neurons and itself. The net value of the neuron  $i$  is described as

$$\text{Net}_{ik}^{(t+1)} = \sum_{j \in N_i} w_{ij} o_{jk}^{(t)} + \theta_i, \tag{2}$$

where  $\text{Net}_{ik}^{(t+1)}$  is the net value of neuron  $i$  associated with class  $k$  in iteration  $t + 1$ ,  $o_{jk}^{(t)}$  is the output state of neuron  $j$  associated with class  $k$  in iteration  $t$ , and  $\theta_i$  is the offset bias fed to the neuron  $i$ . In our approach, the  $\theta$  of all neurons is set to zero. So Eq. (2) becomes

$$\text{Net}_{ik}^{(t+1)} = \sum_j w_{ij} o_{jk}^{(t)}. \tag{3}$$

Each pixel has  $c$  neurons associated with  $c$  clusters to represent the membership degree of each cluster. When the net values of the neurons have been updated in Eq. (3), the outputs of all neurons will be updated depending on the new net values. Following the fuzzy  $c$ -means algorithm, the new output values can be obtained using the following equation:

$$o_{ik}^{(t+1)} = \frac{[\text{Net}_{ik}^{(t+1)}]^{1/q-1}}{\sum_{j=1}^c [\text{Net}_{ij}^{(t+1)}]^{1/q-1}}.$$

The proposed segmentation algorithm is summarized as follows:

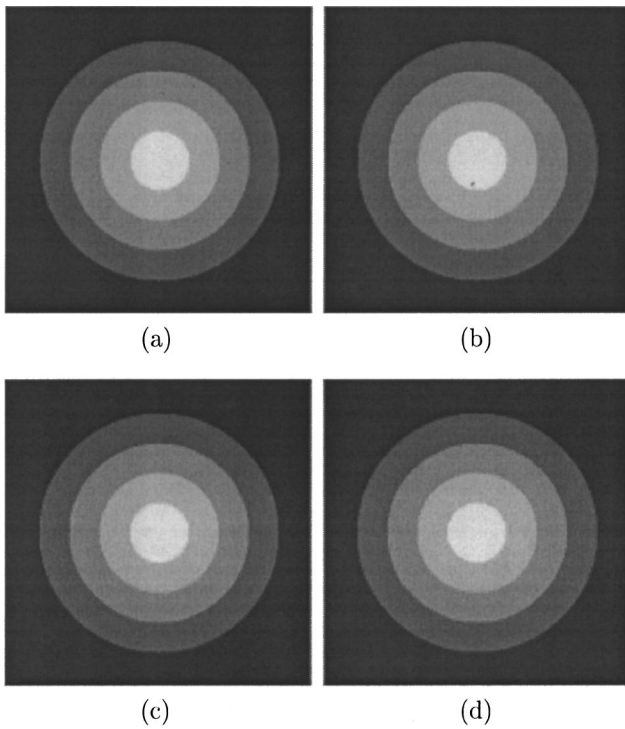


**Fig. 3** The segmentation results with added noise level  $K=20$  using (a) HCM, (b) FCM, (c) CHNN, and (d) the proposed approach.

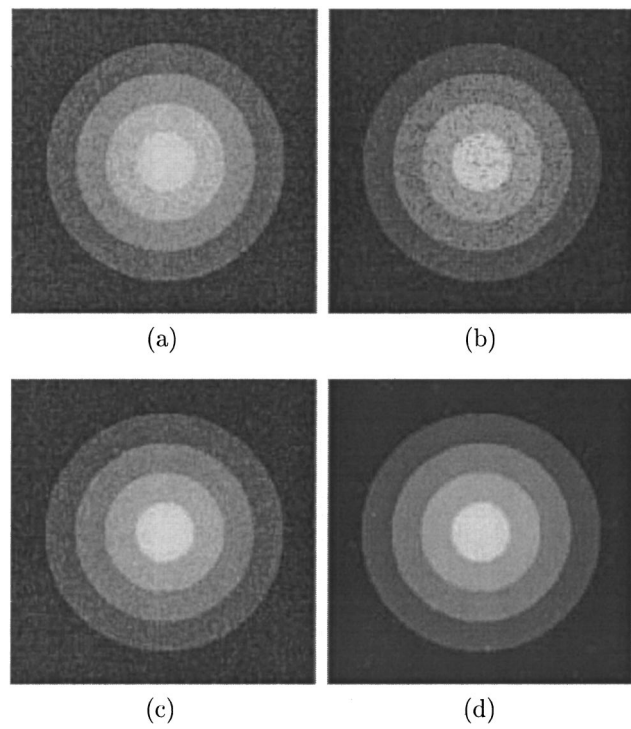


**Fig. 5** The segmentation results with added noise level  $K=25$  using (a) HCM, (b) FCM, (c) CHNN, and (d) the proposed approach.

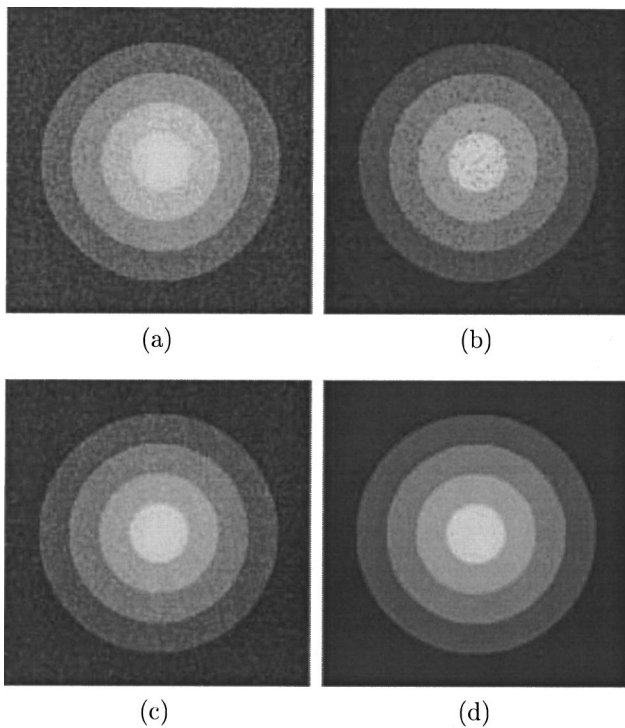


**Fig. 4** The segmentation results with added noise level  $K=23$  using (a) HCM, (b) FCM, (c) CHNN, and (d) the proposed approach.

**Table 1** The number of misclassified pixels and error rate with noise level  $K=20$ .

	HCM	FCM	CHNN	proposed approach
Number of misclassified pixels	0	0	0	0
Error rate	0.00	0.00	0.00	0.00

**Table 2** The number of misclassified pixels and error rate with noise level  $K=23$ .

	HCM	FCM	CHNN	proposed approach
Number of misclassified pixels	31614	5090	9434	59
Error rate	0.4823	0.0776	0.1439	0.0009

**Table 3** The number of misclassified pixels and error rate with noise level  $K=25$ .

	HCM	FCM	CHNN	proposed approach
Number of misclassified pixels	31644	8898	14022	361
Error rate	0.4828	0.1357	0.2139	0.0055

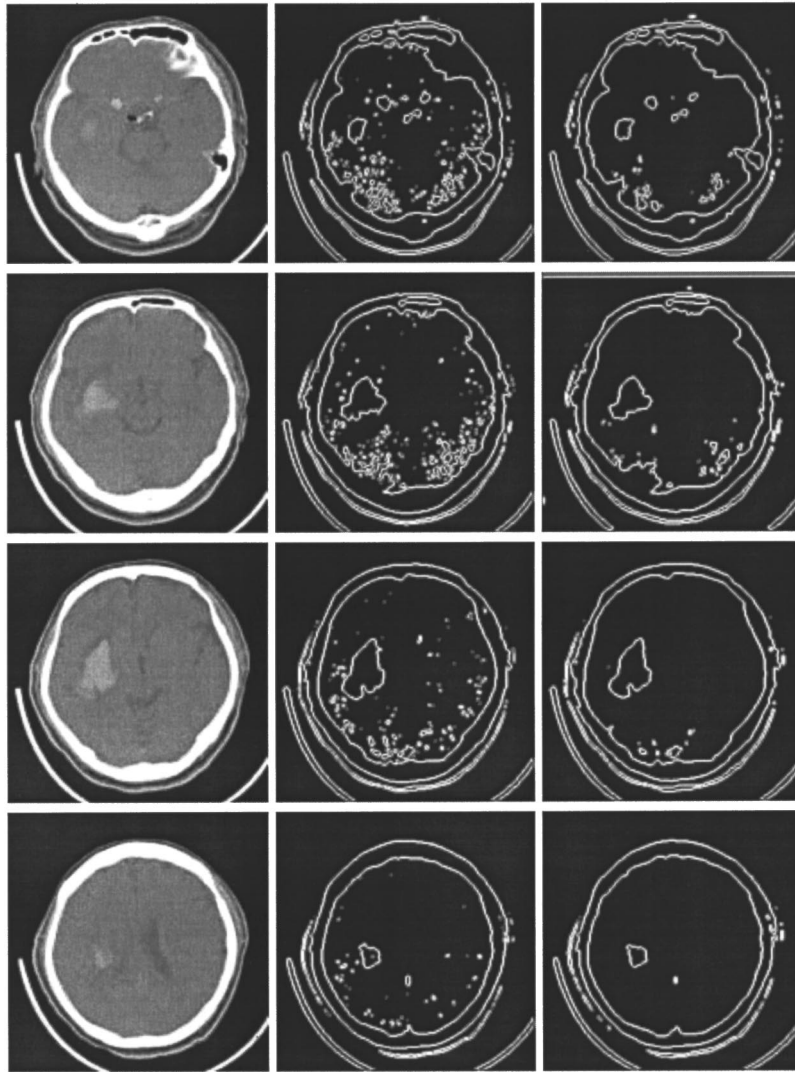


**Fig. 6** The images in the first column are the original images. Images in the second column were obtained by first applying a mean filter to the original images, then applying intensity thresholding. The images in the third column were obtained by the proposed method.

- Step 1. Determine the neighborhood window,  $N$ , and calculate the weights,  $w_{ij}$ ,  $1 \leq i \leq n$ , for a neuron  $j \in N_i$  using Eq. (1).
- Step 2. Initial clustering.
- Step 3. Calculate the net value using Eq. (3).
- Step 4. Update the output states using Eq. (3).
- Step 5. If  $\max_{ik} |o_{ik}^{(t+1)} - o_{ik}^{(t)}| < \epsilon$  then go to Step 6; otherwise  $t = t + 1$  and go to Step 3.
- Step 6. Output the final result using the defuzzification process as
 
$$S_i = k, \quad \text{if } o_{ik} = \max_{1 \leq j \leq c} \{o_{ij}\},$$
 where  $S_i$  is the segmentation label of pixel  $i$ .

#### 4 Simulation and Experiment Results

In our experiments, we used a set of phantom data and medical images to evaluate the performance of the proposed algorithm. The phantom data set based on CHNN<sup>7</sup> was used, as shown in Fig. 2(a), which was produced from

four overlapping disks and the background. An average gray scale for each region was: the average gray value of the background was 30, and from the outer most circle to the center, the average gray values of four disks were 75, 120, 165, and 210, respectively.

The gray scale in each region was not a constant. Suppose that  $\mu$  is the average gray scale in a region. The gray scales in the region were uniformly distributed over the range  $[\mu - k, \mu + k]$ , where  $k$  is a constant. Figures 2(b) through 2(d) are the phantom data sets containing noise with  $K = 20, 23$ , and  $25$ , respectively. We applied the hard  $c$ -means (HCM), fuzzy  $c$ -means (FCM), competitive Hopfield neural network (CHNN), and the proposed approach to process the phantom data sets. Figures 3–5 are the segmentation results with noise levels  $K = 20, 23$ , and  $25$ , respectively. In these figures, parts (a) through (d) are the results segmented by applying HCM, FCM, CHNN, and the proposed approach, respectively. We compared the amount of misclassified pixels and the error rates to evalu-

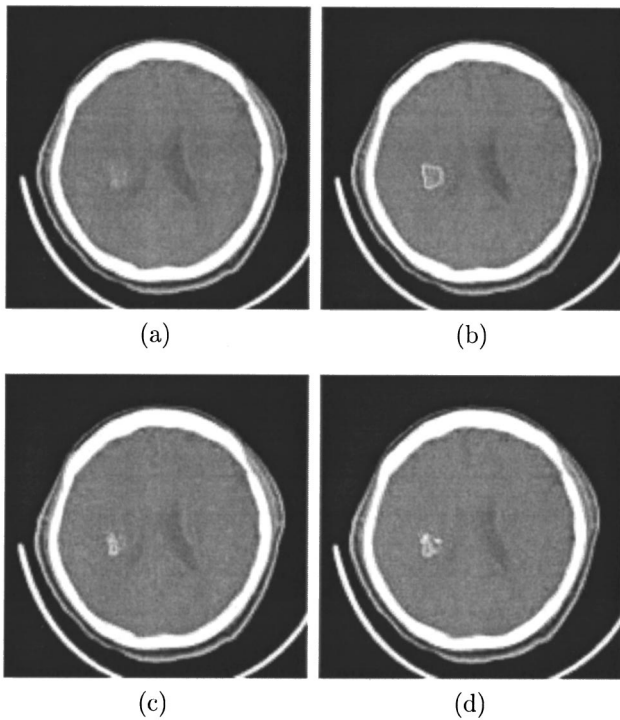


**Fig. 7** (a) The original CT image of human head; (b), (c), and (d) are the segmentation results using the proposed approach, HKM, and FKM, respectively.

ate the performance. Tables 1–3 show the comparison results from these phantom data sets using these four methods. All of the four methods perfectly segmented the objects when the noise level was  $K=20$ . If the noise levels were higher when  $K=23$  and  $25$ , the performance of the proposed approach was better than other three methods, both in perception quality and quantitative comparisons (see Figs. 4, 5, and Tables 2 and 3).

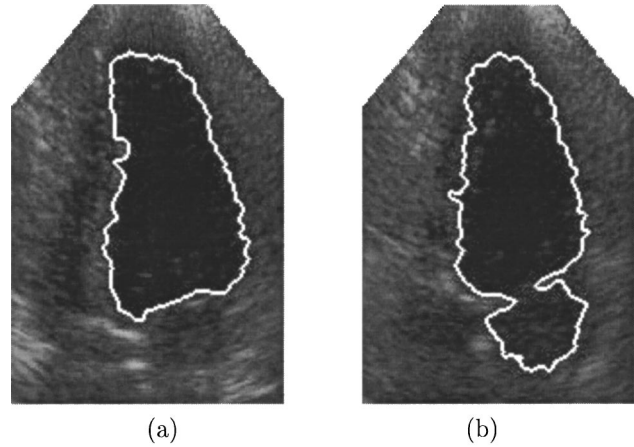


**Fig. 8** (a) and (b) are two echocardiographic images with the boundaries obtained by the proposed approach.

We applied the proposed algorithm to segment the area of interest in medical images. The first was a set of CT images of a head scan. The region of interest in the CT images is a blood clot. The blood clot has higher intensity than the soft tissue. Two experiments were done on this set of images. The first experiment was to compare the proposed method against an intensity thresholding method. When we are partitioning the pixels into two classes, the effect of the proposed method is the same as the intensity thresholding method. The proposed method needs two initial cluster centers, while the thresholding method needs an exact threshold value. When the thresholding method was applied, we first applied a mean filtering to the image. We then carefully chose the best possible threshold to segment the blood clot. The results are shown in Fig. 6. In Fig. 6, the first column shows the original image. The boundary points obtained by using the thresholding method are shown in the second column. The boundary points obtained by using the

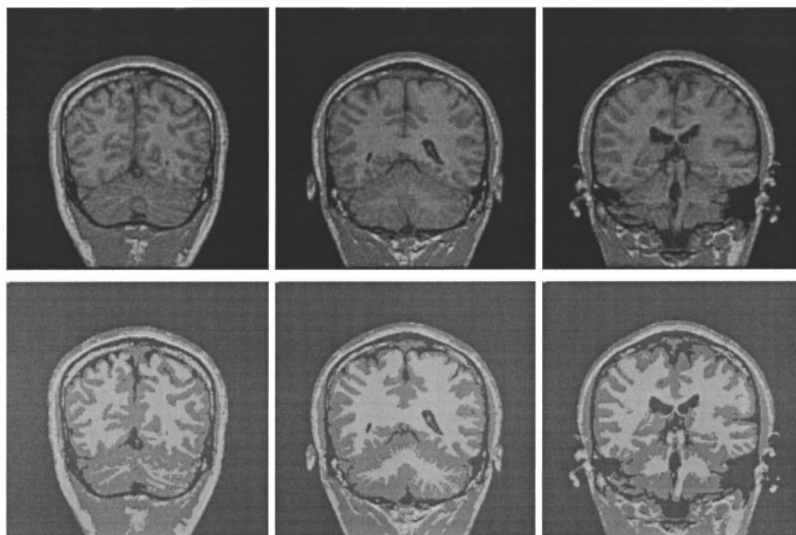


**Fig. 9** The pixels in the MR images are partitioned into four sets. From left to right, each column shows the original image (above) and the processed image (below).

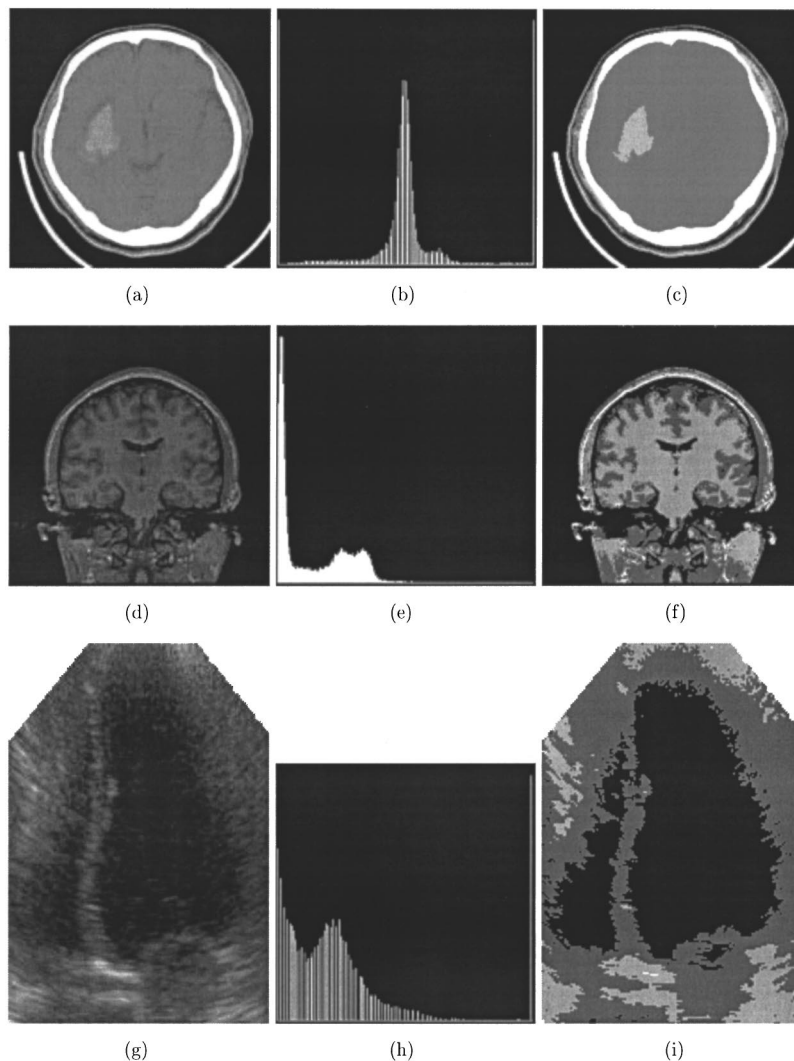


**Fig. 10** (a), (d), and (g) are the original images of (a) CT, (d) MR, and (g) echocardiography; (b), (e), and (h) are the histogram of (a), (d) and (g). (c), (f) and (i) are the segmentation results by first applying the hard *c*-means algorithm for initial clustering, and then applying the proposed approach. The number of cluster centers was, respectively, 5, 4, and 4 for CT, MR, and echocardiographic images.

proposed method are shown in the third column. The proposed method can obtain relatively clean images.

The second experiment was to compare the proposed method with the HCM and FCM. Figure 7(a) is an original CT image of a human head scan. Figure 7(b) shows the blood clot segmented using the proposed approach. We also segmented the blood clot by using HCM and FCM algorithms and show the results in Figs. 7(c) and 7(d). The result obtained by the proposed approach was much better than the other two methods.

We applied the proposed method to classify the pixels in the echocardiographic images. In this experiment, precordial echocardiographic images were used. The region of interest in the echocardiographic images is generally the heart chamber. The heart chamber in the image generally has low intensity. The segmentation of a heart chamber is difficult due to the speckle noise. The boundaries of the segmented results from the proposed approach are shown together with the original images in Fig. 8. These results

show that the proposed approach works well for cardiac ultrasound images.

The next experiment was to classify the pixels in MR images of a human head scan. We classified the pixels into four sets. Figure 9 shows the original images in the first row and the processed images in the second rows. The results show that the proposed method also works well to classify the pixels in MR images.

In the following, we present the results obtained using a two step segmentation method. In the first step, we used the global information to estimate the cluster centers. We then applied the proposed method to classify the pixels into clusters. The first step was carried out using the hard *c*-means algorithm to divide the intensity into clusters. The centers of these clusters then serve as the initial centers for the proposed method. Figures 10(a), 10(d), and 10(g) are the original images of CT, MRI, and echocardiogram. Figures 10(b), 10(e), and 10(h) are, respectively, the histograms of Figs. 10(a), 10(d), and 10(g). Figures 10(c), 10(f)

and 10(i) are the segmented results. The number of cluster centers for the hard  $c$ -means algorithm were, respectively, 5, 4, and 4, for CT, MR, and echocardiographic images. Note that we used five cluster centers for CT images. Five initial cluster centers were needed because the region of interest, the blood clot, is relatively small in the image.

## 5 Conclusion

A new medical image segmentation technique was presented. The global gray-level information was incorporated to perform the initial clustering, and then the local gray-level information was used to construct a fuzzy Hopfield neural network. A fixed weights approach was utilized to reduce the computing time for neural network stabilization. According to our experiments on the phantom data set, the performance of the proposed approach is much better than the hard  $c$ -means, fuzzy  $c$ -means, and CHNN methods. Our experiments on the real medical images, demonstrated good results, which were either the initial cluster centers estimated by the hard  $c$ -means algorithm or the initial cluster centers obtained from the prior knowledge. However, deciding the best number of cluster centers for the hard  $c$ -means method becomes another problem. Our experiments show that increasing the number for cluster centers for the hard  $c$ -means method can achieve good result.

## Acknowledgment

This work was supported under contracts NSC-88-2213-E-009-019 and NSC-89-2213-E-009-098, National Science Council, Taiwan, Republic of China.

## References

1. K. S. Fu and J. K. Mui, "A survey on image segmentation," *Pattern Recogn.* **13**, 3–16 (1981).
2. N. R. Pal and S. K. Pal, "A review on image segmentation techniques," *Pattern Recogn.* **26**, 1277–1294 (1993).
3. R. C. Gonzalez and R. E. Woods, *Digital Image Processing*, Addison-Wesley, Reading, MA (1992).
4. A. P. Dhawan and L. Arata, "Segmentation of medical images through competitive learnings," *Comput. Methods Programs Biomed.* **40**, 203–215 (1993).
5. W. C. Lin, E. C. Tsao, and C. T. Chen, "Constrain satisfaction neural networks for image segmentation," *Pattern Recogn.* **25**(7), 679–693 (1992).
6. C. T. Chen, E. C. Tsao, and W. C. Lin, "Medical image segmentation by a constraint satisfaction neural network," *IEEE Trans. Nucl. Sci.* **38**(2), 678–686 (1991).
7. K. S. Cheng, J. S. Lin, and C. W. Mao, "The application of competitive Hopfield neural network to medical image segmentation," *IEEE Trans. Med. Imaging* **15**(4), 560–567 (1996).
8. J. S. Lin, K. S. Cheng, and C. W. Mao, "A fuzzy Hopfield neural network for medical image segmentation," *IEEE Trans. Nucl. Sci.* **43**(4), 2389–2398 (1996).
9. J. S. Lin, K. S. Cheng, and C. W. Mao, "A modified Hopfield neural network with fuzzy  $c$ -means technique for multispectral MR image segmentation," *Proc. IEEE Int. Conf. Image Processing*, 327–330 (1996).
10. G. Coppini, R. Poli, and G. Valli, "Recovery of the 3-D shape of the left ventricle from echocardiographic images," *IEEE Trans. Med. Imaging* **14**(2), 301–317 (1995).
11. Y. Zhu and H. Yan, "Computerized tumor boundary detection using a Hopfield neural network," *IEEE Trans. Med. Imaging* **16**(1), 55–67 (1997).
12. J. C. Bezdek, *Pattern Recognition with Fuzzy Objective Function Algorithm*, Plenum, New York (1981).



**Chwen-Liang Chang** received the BS degree in computer science from Chung-Cheng Institute of Technology, Taiwan, in 1988. He is currently a PhD student in the computer and information science department at National Chiao-Tung University. His research interests are in the areas of image processing, computational geometry, medical imaging, deformable models, and neural networks.

**Yu-Tai Ching** received his BS degree in industrial engineering from Tsing Hua University, Taiwan, in 1980, and MS and PhD degrees in computer science from Northwestern University, Evanston, Illinois, in 1983 and 1987. His research interests are medical image analysis, computer graphics, design, and analysis of algorithms.